

# Quality Related Effects of the Preheating Temperature on Laser Melted High Carbon Content Steels

Livia Zumofen<sup>(✉)</sup>, Christian Beck, Andreas Kirchheim,  
and Hans-Jörg Dennig

Centre for Product and Process Development,  
Zurich University of Applied Sciences, Winterthur, Switzerland  
livia.zumofen@zhaw.ch

**Abstract.** Additive manufacturing technology selective laser melting (SLM) is an emergent technology allowing generation of complex metal parts layer by layer. During the past years the range of available and processable materials for SLM has been widely extended. However, there is still a lack of SLM processable high carbon content steels. In the fields of machine elements, especially in advanced cutting tools a large potential of laser melting is identified regarding function integration, topology optimisation and implementation of bionic concepts. In these fields of application high carbon content steels are frequently used. The M2 High Speed Steel (HSS) is a high carbon content steel that belongs to the group of tool steels. As other high carbon content steels, M2 HSS tends to a high susceptibility to cracking. Therefore, the strongly pronounced temperature gradients occurring during the laser melting process lead to part deformation and crack formation. Heating of the SLM baseplate represents a promising approach to reduce temperature gradients and internal stresses. In the present study the quality related effects of reduced temperature gradients on SLM parts were evaluated using a baseplate heating system. Optimized process parameters allowed a stable processing of M2 HSS leading to a relative part density of 99%. Residual stresses decreased with increasing baseplate temperature by trend.

**Keywords:** High carbon content steel · Selective laser melting · M2 HSS · Tool steel · Internal stresses

## 1 Introduction

Selective laser melting (SLM) is an emergent additive manufacturing technology, which allows layer-wise generation of complex metal parts based on 3D models [1]. The enormous market expansion of SLM machines in the last years points out the increasing importance of additive manufacturing, particularly in the processing of metals [2]. Due to the new design opportunities offered by SLM, great potential is identified in function integration, topology optimisation and implementation of bionic concepts [1, 3]. In the fields of machine elements, especially in advanced cutting tools high carbon content steels are frequently used.

The M2 High Speed Steel (HSS) is a high carbon content steel that belongs to the group of tool steels and is widely used for cutting tools, due to its high hardness, high wear resistance and relatively high toughness [4]. Therefore, processing of M2 HSS is of high interest for advanced tools with high complexity e.g. including internal cooling or lubrication channels. However, high carbon content steels do not yet belong to the standard materials for laser melting, due to their high susceptibility to cracking and deformation when processed with SLM [4–6]. The strongly pronounced temperature gradients occurring during the SLM process are associated with high cooling rates inducing residual stresses [4, 5]. Residual stresses may ultimately lead to warping, part deformation and crack formation. These factors complicate the SLM processing of M2 HSS and currently limit the achievable part quality.

By analogy to laser welding of high carbon content steels, where preheating is a necessity, heating of the SLM baseplate represents a promising approach to reduce occurring temperature gradients. Preliminary studies showed that increased baseplate temperature of up to 200 °C is capable of reducing crack formation in M2 HSS [4, 5]. However, the direct effect of the baseplate temperature on residual stresses remains unknown.

The present work includes a parameter study with focus on scan velocity to allow a stable laser melting process of M2 HSS leading to low porosity. To reduce thermal gradients and internal stresses, a preheating system to heat the baseplate up to 400 °C is applied. Evaluation of porosity and residual stresses in relation to the baseplate temperature represent the main focus.

## 2 Methods and Experiments

### 2.1 Powder

Inert gas atomized M2 HSS powder with 0.83% carbon content was supplied from SANDVIK OSPREY LTD. As shown in Fig. 1, the powder has a prevalent spherical shape with small satellites, especially at the larger fraction. The powder has a Gaussian particle size distribution with particle size of 15–48 µm.

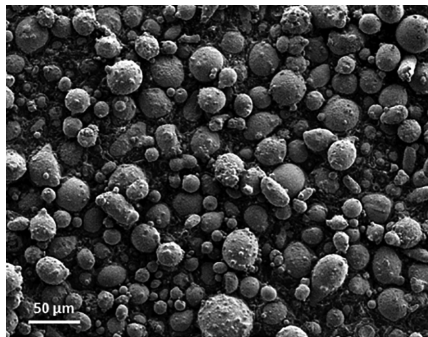


**Fig. 1.** SEM image of used M2 HSS powder.

## 2.2 Laser Melting

Selective laser melting is a powder bed based additive manufacturing technology that allows generation of metal parts with low porosity layer by layer. For each layer, a thin powder layer is added, which is selectively melted and connected to the underlying layer, according to 3D data (Fig. 2). Then, the baseplate is lowered and the aforementioned procedure repeated for subsequent layers until the build is completed.

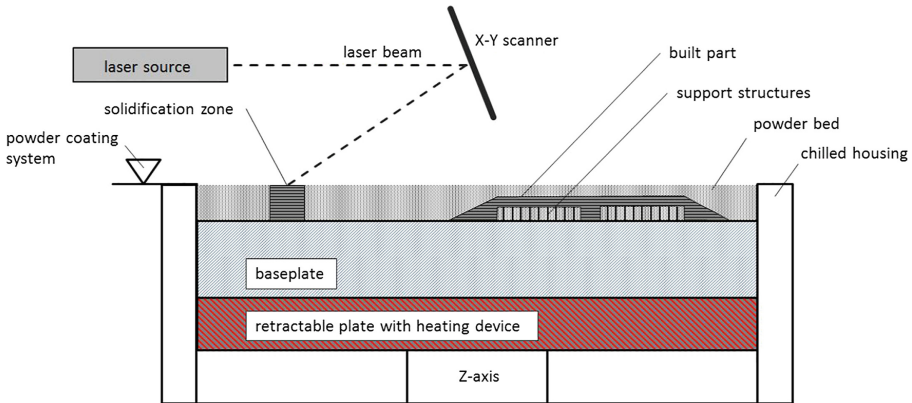


**Fig. 2.** Schematic representation of the SLM process including the baseplate heating system.

Experiments were carried out on a Renishaw AM 250 laser melting system, which is equipped with a 200 W fiber laser operated in pulsed mode. The beam has a  $M^2$  of  $< 1.1$  and a spot diameter of  $70 \mu\text{m}$ . Argon was used as inert gas with an oxygen threshold of maximum 1000 ppm. An additional baseplate heating device was integrated in the Renishaw AM 250 laser melting system (Fig. 2), which is located below the baseplate.

In order to evaluate effects of scan velocity and baseplate temperature on the part density, cubic specimens were manufactured (2.3). On the basis of specifically designed cantilevers, residual stresses were evaluated with the previously optimized parameter set (2.4). All specimens were manufactured with meander scan strategy,  $40 \mu\text{m}$  layer thickness, 200 W laser power and  $80 \mu\text{m}$  hatch space. Scan velocity varied between 500 mm/s and 1500 mm/s and baseplate temperature between  $160 \text{ }^\circ\text{C}$  and  $400 \text{ }^\circ\text{C}$  for cubic specimens. Cantilevers were manufactured with optimized scan velocity of 750 mm/s and baseplate temperatures of  $160 \text{ }^\circ\text{C}$ – $400 \text{ }^\circ\text{C}$  (2.4).

## 2.3 Porosity

Low porosity is an essential quality criterion of SLM parts, due to its direct relation to mechanical properties and the demand for comparable strength to bulk material [8]. Porosity is strongly dependent on process parameters and process conditions. Furthermore, an adequate energy input into the powder layer is needed in order to achieve

complete melting and generate a homogenous melt track. Therefore, optimum process parameters are required in order to allow a stable SLM process resulting in high part density.

Thereby, the energy density ( $E_D$ ) represents a common term to describe the energy input of the laser into a defined volume of material [9], whereas the most important parameters are taken into account (Eq. 1). These include the laser power ( $P_{Laser}$ ), scan velocity ( $v_{Scan}$ ), hatch space ( $s_{Hatch}$ ) and layer thickness ( $t_{Layer}$ ).

$$E_D = \frac{P_{Laser}}{v_{Scan} \cdot s_{Hatch} \cdot t_{Layer}} \quad (1)$$

To evaluate the effects of scan velocity on part density when processing the M2 HSS, specimens with  $10 \times 10 \times 10 \text{ mm}^3$  dimension were manufactured with base parameters as mentioned in (2.2) and varying scan velocity of 500 mm/s–1500 mm/s at 400 °C baseplate temperature. For each set of parameters three specimens were manufactured. As the scan velocity contributes to the energy density, the consequent energy density decreases accordingly with increasing scan velocity (Table 1).

**Table 1.** Evaluated field of scan velocity and corresponding energy density at 400 °C baseplate temperature.

Sample	Scan velocity [mm/s]	Energy density [Ws/mm <sup>3</sup> ]
1	1500	42
2	1375	45
3	1250	50
4	1125	56
5	1000	63
6	875	72
7	750	83
8	625	100
9	500	125

The density was evaluated according to the archimedes' principle following the VDI 3405 guideline [10]. Specimens were analyzed using a KERN ABJ 220-4NM measuring device with water as displacement fluid. The relative density was determined based on the ASTM M2 standard density of 8.138 g/cm<sup>3</sup> [11].

## 2.4 Temperature Gradient Induced Residual Stresses

Previous studies showed the applicability of cantilevers to evaluate residual stresses induced by SLM in various process conditions [12, 13]. Therefore, investigation of residual stresses in the solidified material is carried out using defined cantilever constructions. Subsequent separation of the support structures creates a controlled deformation in the form of deflection. These deflections provide insight into presence of residual stresses. The separation was implemented with a band saw. Subsequent deflections in Z-axis were assessed using a Mitutoyo 192–106 height measuring device.

Cantilevers with two branches are designed and slightly modified to facilitate reproducible support separation (Fig. 3). The cantilever consists of a massive centrally located socket and two symmetrically arranged and supported branches. Supports are 0.5 mm thick arranged with 0.8 mm spacing. The endings of both branches are firmly connected to the base plate, to avoid spontaneous detaching prior to separation. Cantilevers were manufactured at 160 °C, 240 °C, 320 °C and 400 °C with all other parameters remaining identical. At each baseplate temperature, one cantilever per branch thicknesses of 1 mm, 1.5 mm, 2 mm and 4 mm was manufactured. The cantilever dimensions were identical except for the thickness of the branches.

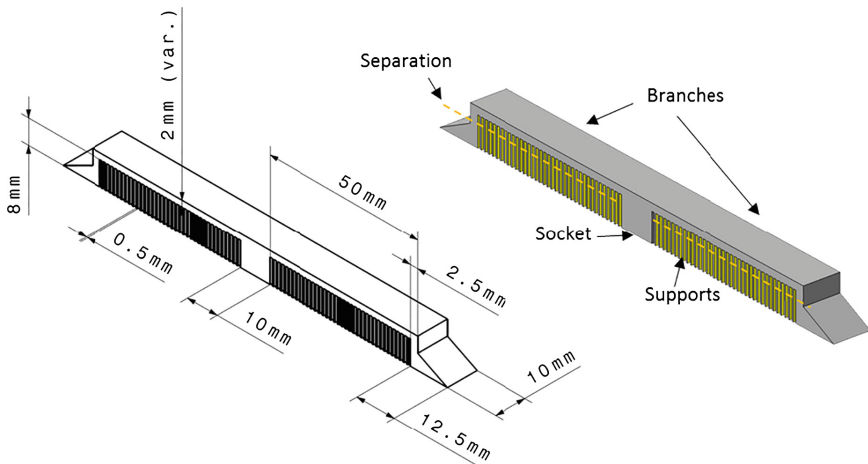


**Fig. 3.** Dimensions of cantilevers with two branches to evaluate residual stresses.

### 3 Results and Discussion

#### 3.1 Process Parameters

Investigated specimens possessed a relative density between 98.2% and 99.2%. As displayed in Fig. 4, the density increased with decreasing scan velocity by trend, peaking at around 750–625 mm/s. Considering the melt track homogeneity, scan velocity of 500 mm/s led to strongly pronounced irregularities (Fig. 5).

Scanning electron microscopic evaluation showed homogenous melt tracks at 750 mm/s scan velocity (Fig. 6A). Therefore, scan velocity of 750 mm/s and corresponding energy density of 83 Ws/mm<sup>3</sup> led to both, high part density (Fig. 4) and homogenous melt tracks (Fig. 6A). Besides that, no effect of the baseplate temperature on the specimen density has been recognized (Fig. 6B). Therefore, further experiments were carried out based on the base parameters described in 2.2 and a scan velocity of 750 mm/s.

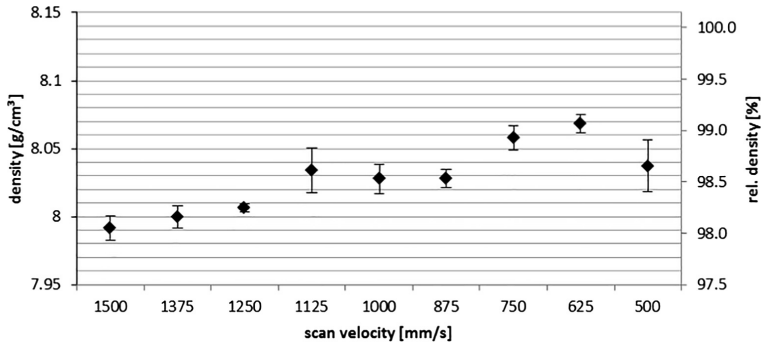


**Fig. 4.** Absolute and relative density of cubic specimens in relation to scan velocity at 400 °C base plate temperature. Values represent mean  $\pm$  standard deviation.

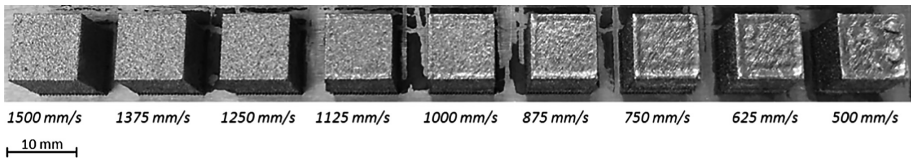


**Fig. 5.** Top view of cubic specimens with varying scan velocity of 1500 mm/s–500 mm/. Baseplate temperature: 400 °C.

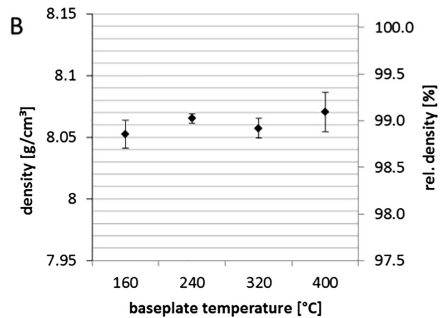
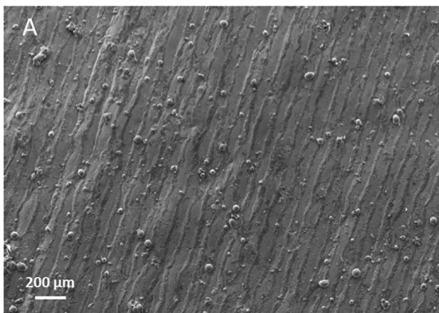


**Fig. 6.** SEM image of top surface of a cubic specimen manufactured with 750 mm/s scan velocity and 400 °C baseplate temperature (A) and density in relation to baseplate temperature. Values represent mean  $\pm$  standard deviation (B).

Metallographic cross-sections in horizontal and vertical direction demonstrated a homogenous distribution of spherical shaped pores within specimens manufactured with 750 mm/s scan velocity and 400 °C baseplate temperature (Fig. 7).

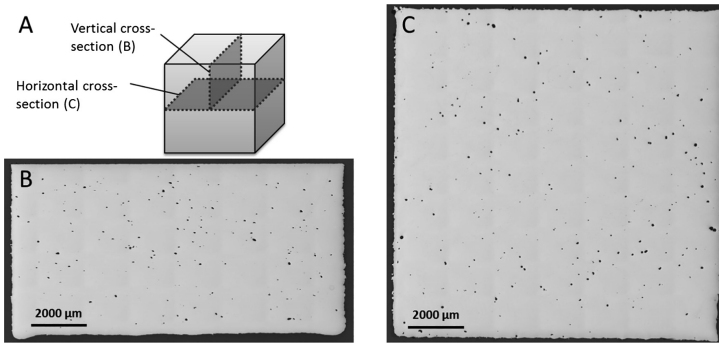


**Fig. 7.** Cross-sections of cubic specimens (A) in vertical (B) and horizontal (C) direction.

### 3.2 Effect of Baseplate Temperature on Residual Stresses

As demonstrated in Fig. 8, manufactured cantilevers already contained imperfections, deformations or cracks prior to separation from supports. Early cracking was exclusively observed at baseplate temperatures of 160 °C and below. However, imperfections and deformations were present at baseplate temperatures up to 400 °C. Some of these imperfections have even led to cracking and complete failure during separation, especially at 1 mm branch thickness. Therefore, cantilevers of 1 mm branch thickness were not further pursued.

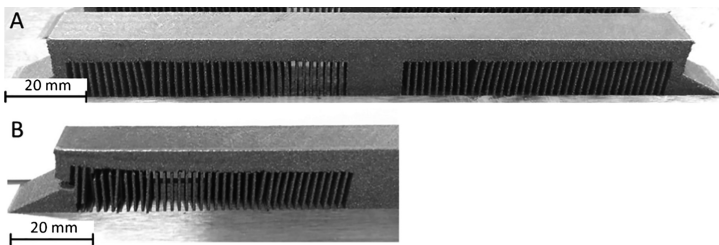


**Fig. 8.** Cantilevers with 4 mm branches and imperfections at 240 °C baseplate temperature (A); Early deformations and cracks prior to separation at 160 °C baseplate temperature (B).

Deformations of evaluated cantilevers at baseplate temperatures of 160 °C–400 °C are shown in Fig. 9. In consideration of 1.5–4 mm branch thicknesses, the deflection decreased with increasing thickness. The two branches of all cantilevers showed slight deviations between each other. On one hand occurring deviations may be attributed to inconsistent presence of imperfections, but also to temperature differences on the heated baseplate. At 400 °C baseplate temperature negative deflections of cantilever branches with 2 mm and 4 mm thickness were observed. The change of positive to negative deflection from 320 °C to 400 °C indicates a change of tensile stresses to compressive stresses. A similar phenomenon was also observed on H13 tool steel [7].

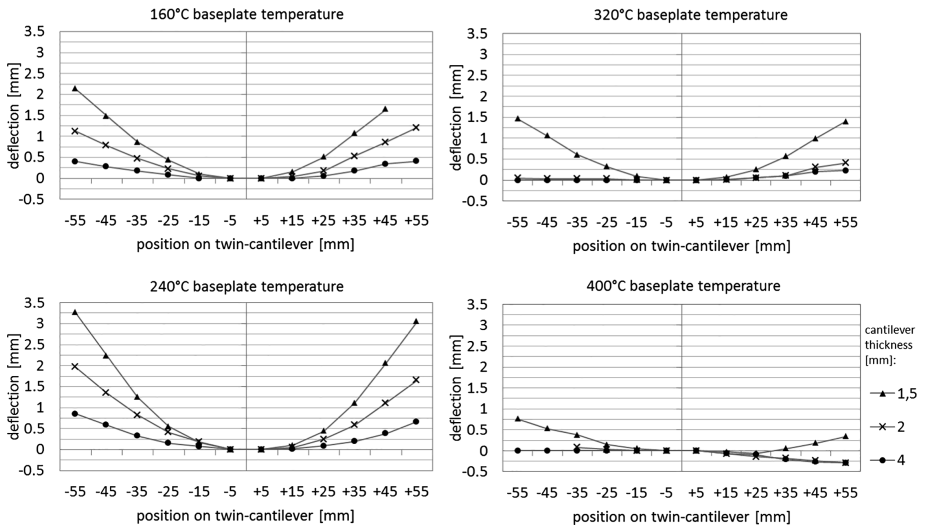


**Fig. 9.** Deflection of cantilevers with 1.5 mm, 2 mm and 4 mm thickness at different baseplate temperatures of 160–400 °C.

As demonstrated in Fig. 10, the deflection of cantilever branches of 4 mm thickness decreased with increasing baseplate temperature above 240 °C. Therefore, residual stresses are expected to decrease with increasing baseplate temperatures above 240 °C accordingly.

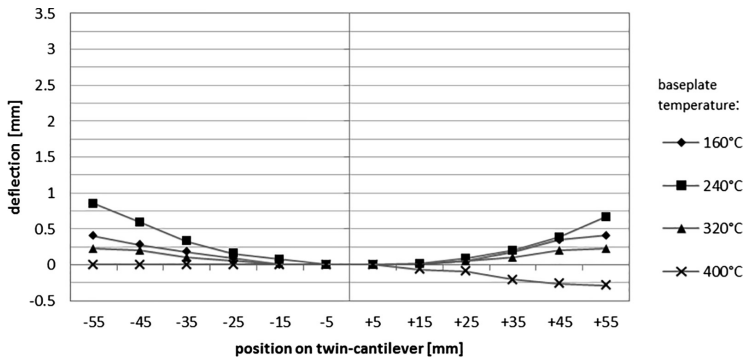


**Fig. 10.** Influence of temperature on deflection of cantilevers with 4 mm thickness.

Porosity is reported to have an influence on residual stresses [14]. As porosity has been found to be independent of the baseplate temperature within the investigated range (Fig. 6), no such effect is expected to interfere with the aforementioned finding. In contrary, deflection of the cantilever manufactured at 160 °C baseplate temperature was lower than the one at 240 °C (Fig. 10). It is suspected that this result originates



from internal stresses above the strength of the material resulting in early relieve of stresses by deformation (Fig. 8B) and micro cracking during manufacturing, lowering the final deflection of the cantilever.

Based on the aforementioned findings, demonstrators of drillers with internal cooling channels were successfully manufactured with 750 mm/s scan velocity and 400 °C baseplate temperature (Fig. 11).

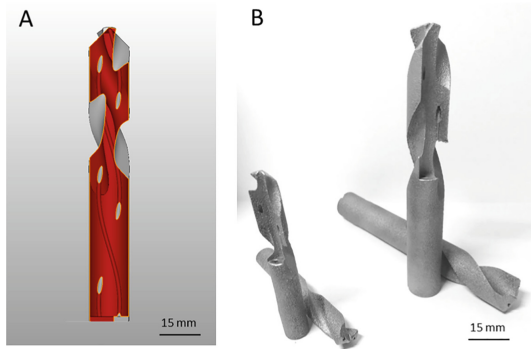


**Fig. 11.** Sectional view of the 3D model of a driller with internal cooling channels (A) and laser melted M2 HSS drillers (B).

## 4 Conclusions

Present results showed that M2 HSS may be processed using SLM and a baseplate heating system. Furthermore, the high potential of baseplate heating to reduce internal stresses has been demonstrated. However, residual stresses, imperfections and slight deformations still remained at 400 °C baseplate temperature under investigated conditions. Internal stresses are assumed to be increasingly critical at decreasing feature sizes, especially in parts where a combination of filigree and massive structures is present. By further optimization of process parameters a further reduction of internal stresses, but also porosity are suspected. This includes investigation of the effects of hatch spacing on part porosity and internal stresses. Besides that, investigation of formation of micro cracks and microstructure is of high interest. Further work is also recommended to focus on the characterization of the baseplate heating system and temperature distribution within the build part as a function of build height. It is suggested also to take a combination of the baseplate heating system with additional pre heating systems into account, e.g. infrared radiators to achieve a homogenous pre-heating temperature throughout the part as well as on the actual powder layer.

**Acknowledgements.** The authors acknowledge Renishaw plc. for supporting this project.

## References

1. Gebhardt, A.: Generative Fertigungsverfahren. Additive manufacturing und 3D-Drucken für Prototyping – Tooling – Produktion. 4. neu bearb. und erw. Auflage. Carl Hanser Verlag, München (2013)
2. Wohlers, T., Caffrey, T.: Wohlers Report 2015. 3D-Printing and Additive Manufacturing State of the Industry – Annual Worldwide Progress Report. Wohlers Associates, Fort Collins/US (2015)
3. Gibson, I., Rosen, D., Stucker, B.: Additive manufacturing technologies. 3D Printing, Rapid Prototyping, and Direct Digital Manufacturing. Springer Verlag, Berlin (2010)
4. Kempen, K., Thijs, L., Buls, S., van Humbeeck, J., Kruth, J.-P.: Lowering Thermal gradients in selective laser melting by pre-heating the baseplate. In: Bourell, D.L. (ed) Proceedings of the 2nd Solid Freeform Fabrication Symposium, Austin, TX, pp. 12–24, August 2013. University of Texas at Austin (2013)
5. Taha, M.A., Yousef, A.F., Gany, K.A., Sabout, H.: On Selective Laser Melting of Ultra High Carbon Content Steel: Effect of Scan Speed and Post Heat Treatment. Materialwissenschaften und Werkstofftechnik. Wiley-VCH Verlag GmbH, Weinheim (2012)
6. Liu, Z.H., Chua, C.K., Leong, K.F., Kempen, K., Thijs, L., Yasa, E., van Humbeeck, J., Kruth, J.-P.: A preliminary investigation on selective laser melting of M2 high speed steel. In: 5th International Conference on Advanced Research in Virtual and Rapid Prototyping, Leira, Portugal (2011)
7. Mertens, R., Vrancken, B., Holmstock, N., Kinds, Y., Kruth, J.-P., van Humbeeck, J.: Influence of powder bed preheating on microstructure and mechanical properties of H13 tool steel SLM parts. In: 9th International Conference on Photonic Technologies – Lane 2016, Physics Procedia, vol. 83, pp. 882–890. Elsevier (2016)
8. Yap, C.Y., Chua, C.K., Dong, Z.L., Liu Z.H., Zhang D.Q., Loh L.E., Sing S.L.: Review of selective laser melting: materials and applications, Applied Physics Reviews (2015)
9. Kruth, J.P., Vandenbroucke, B., Van Vaerenbergh, J., Naer, I.: Rapid manufacturing of dental prostheses by means of selective laser sintering/melting. In: Proceedings of the AFPR, S4, (2005)
10. VDI 3405 Part 3, Additive manufacturing processes, rapid manufacturing – Design rules for part production using laser sintering and laser beam melting. Beuth-Verlag, Berlin (2015)
11. OTAI Special Steel Co. Ltd. <http://www.astmsteel.com/product/m2-tool-steel-1-3343-hs-6-5-2c-skh51/> Accessed 13 Apr 2017
12. Buchbinder, D., Schilling, G., Meiners, W., Pirch, N., Wissenbach, K.: Untersuchung zur Reduzierung des Verzugs durch Vorwärmung bei der Herstellung von Aluminiumbauteilen mittels SLM. RTejournal – Forum für Rapid Technologie (2011)
13. Töppel, T., Müller, B., Hoeren, K. P. J., Witt, G.: Eigenspannungen und Verzug bei der additiven Fertigung durch Laserstrahlschmelzen., pp. 176–186 Schweißen und Schneiden 68, Heft 4 (2016)
14. Mercelis, P., Kruth, J.-P.: Residual stresses in selective laser sintering and selective laser melting. In: Rapid Prototyping Journal, pp. 254–265 (1995)